Chapter 4

Synthesis, antioxidant activity and electrochemical behavior of carbon nanomaterials from plant seeds

In this chapter, synthesis of carbon nanomaterials (CNMs) of different morphologies such as nanospheres, nanocubes and nanoparticles by pyrolysis from plant seeds were described. A total of eight plant seeds [Krishnachura or gulmohar *(Delonix regia)*, Bean *(Phaseolus sp.),* Castor *(Ricinus communis)*, Lai (*Brassica juncea*), Denga (*Amaranthus spinosus*), Chandan or Sandalwood (*Santalumsp*.), Kanchan (*Bauhinia acuminata*), Tishi (*Linum usitatissimun*)] and two seed coats [Castor *(Ricinus communis)*, Mahogany (*Swietenia mehogoni*)] were used as precursors for the production of CNMs under catalyst free conditions. Antioxidant efficacy and electrochemical behaviour of a few select synthesised CNMs have been reported.

4.1. Introduction

During the past few years, carbonnanomaterials derived from natural or biological precursor have drawn immense attention across the world because of their particular microstructures, unusual properties and potential applications in different fields ranging fromdrug delivery, heterogeneous catalysis, hydrogen storage, chemical

sensors and encapsulation of support to electrode materials [1-5]. The major processing route for such material is catalytic decomposition of carbon rich molecules, such as methane, acetylene, benzene, xylene, toluene, carbon monoxide etc. by chemical vapor deposition (CVD) [6-8]. In the past decade, carbon nanostructures of different shapes were synthesizedand properties investigated. The studies on the synthesis of spherically shaped carbon particles have becometopical in the last few years [9-12]. Thespherical carbon nanostructured materials have been found in variety of forms, such ascarbon nano-onions[13,14],multiwalled carbon nanobeads [15], carbon nanospherules with uniform nanopores[16],nanoballs [17], carbon pearls, hollow nanospheres [18] etc.The increasing interests in such materials is due to their high strength, high thermal resistance, lightweight and conductivity and ability to be used in high strength composites, catalyst carriers, lubricants, electronic devices and as wear resistant materials [19].

In the backdrop of this, the goal of the present chapter is to explore the viability of differentplant seeds as precursor for the synthesis of CNMs under catalyst free conditions and to investigate the antioxidant efficacy and electrochemical behaviour of the as-obtained nanomaterials.

4.2. Carbon nanospheres (CNS) from seeds of a tropical plant, *Delonix regia*

4.2.1.Materials

The seeds of *Delonix regia* (**Fig.4)**, a tropical ornamental plant were collected from the plains of north-eastern region of India during May and June 2012. The seeds were thoroughly washed, sun dried, crushed and used as precursor to synthesize CNS. Locally known as *Krishnachura* or *Gulmohar*, this plant belongs to Caesalpiniaceaefamily. It serves as useful shade tree in tropical climatic conditions.

Fig.4.1. Photographs of **(a)** *Delonix regia* plant and **(b)***Delonix regia* seeds

4.2.2. Synthesis of carbon nanospheres

Spherical carbon nanoparticles were produced from the dried and crushed seeds of *Delonix regia* by pyrolysis in a CVD furnace. A quartz boat loaded with the precursor (~10 g) inserted in a horizontal quartz tube was placed in the furnace. The tube was initially flushed with argon gas in order to eliminate air from the tube and then purged at a flow rate of $6cm^3$/min. The furnace was heated to 800^0C at a rate of 7^0C per minute for 2 hours to complete the process of pyrolysis. The system was then allowed to cool to room temperature under inert condition and the black powder so formed were collected from the quartz boat and analysed (yield 2.6 g).

4.2.3. Results and discussion

The as-obtained carbon nanosphere black powder is air stable for months and can be brought into dispersion readily in aqueous and organic solvents (methanol, ethanol) by ultrasonication. The yield of the material was found to be around 25% by weight of the initial biomass.

4.2.3.1. Scanning electron microscopy

The scanning electron microscopy is used to study the external morphology of the as obtained materials. The SEM micrographs**(Fig.4.2.(a))** revealed the presence of uniform monodispersed spherical nanoparticles. The particle size distribution calculated using ImageJ software showed that the maximum particles are in the range of 20-80 nm.

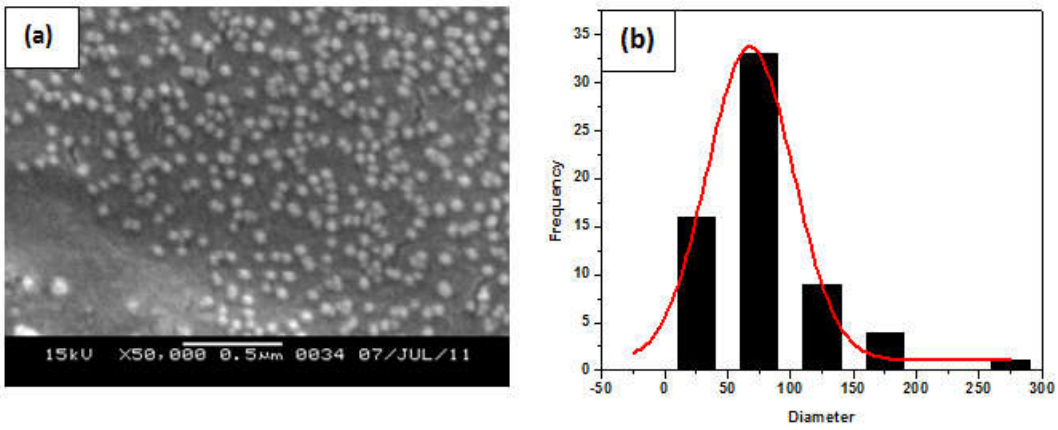

Fig.4.2.(a) SEM micrograph of as prepared carbon nanospheres **(b)** histogram showing average particle size

4.2.3.2. Transmission electron microscopy

The TEMmicrographs showed the presence of monodispersed carbon nanospheres of 42 nm diameter (**Fig.4.3. (a,b)**). From HRTEM image (**Fig.4.3. (c)**), the lattice fringes were observed to be at interplanar distance of 0.33 nm which correspond to (002) plane of graphitic carbon. The concentric ring pattern in SAED attested the graphitic nature of the material (**Fig4.3. (d)**). The graphene sheets that form carbon nanospheres are usually unclosed shells with waving flakes that follow the curvature of the sphere generating some open edges at the surface. Such 'dangling bonds' are quite reactive ensuring high chemical activity [20].

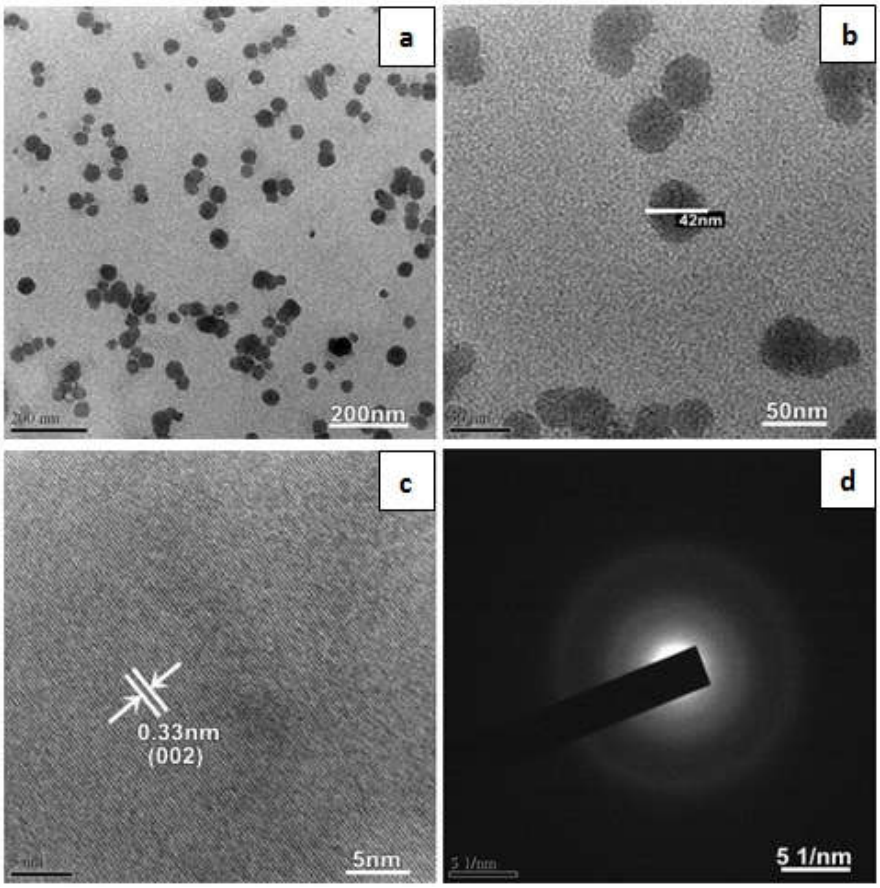

Fig.4.3. (a,b) TEM images **(c)** HRTEM image and **(d)**SAED pattern of the carbon nanospheres obtained from the seeds of *Delonix regia*

4.2.3.3. Energy dispersive spectroscopy (EDS)

The Energy dispersive spectroscopy is used to study the composition of the as obtained materials. The EDS (**Fig.4.4 (a)**) revealed the occurrence of carbon as the

major constituent along with minor contributions from oxygen, magnesium, phosphorus, potassium and calcium.

4.2.3.4. Powder X-ray diffraction study

The powder XRD pattern of the as-obtained CNS (**Fig.4.4 (b)**) showed two major Bragg peaks at 2θ = 26^0 and 44^0corresponding to the (002) and(101) planes, respectively, and few other reflections for (100), (102), (004) and (103) plane of hexagonal graphitic carbon possessing $P6_3/mmc$ space group (JCPDS Card No. 23-0064). The broad nature of the peaks suggests a lesser long range structural order. The interlayer spacing (d_{002} = 0.33nm) found by XRD is consistent with that obtained (d_{002} ~ 0.33 nm) from HRTEM and is characteristic of CNS.

4.2.3.5.Raman Spectroscopy

The graphitic nature was further evidenced by Raman Spectroscopy. The Raman spectrum (**Fig.4.4(c)**) of the CNS exhibited characteristic first order D- and G-bands of graphitic carbon at 1333cm^{-1} and 1598cm^{-1}, respectively. The G band corresponds to the tangential stretching (E_{2g}) mode of the highly oriented pyrolytic graphite. The D-peak assigned to A_{1g} mode originates from the disorder in the sp^2-hybridized carbon and indicates a lattice distortion in the graphitic carbon [21, 22]. The I_D/I_G ratio was found to be 0.91 (<1) indicating a higher degree of graphitization in the material[21].

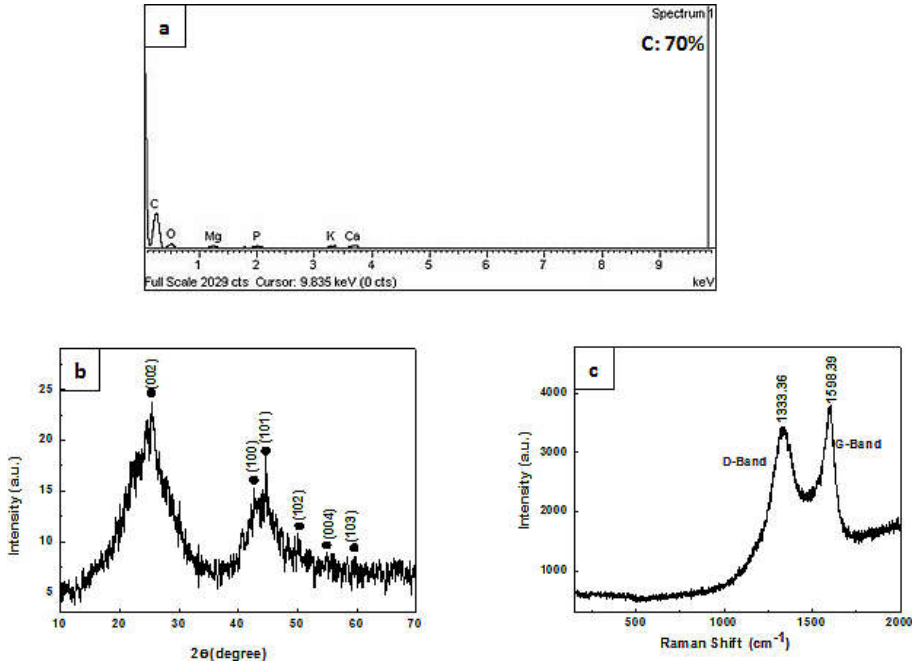

Fig.4.4.(a) EDS **(b)** XRD pattern **(c)** Raman spectrum of the nanospheres obtained from theseeds of *Delonix regia.*

4.2.3.6. Electrochemical behaviour

Energy storage and conversion is one of the important application domains of carbon nanospheres [23]. Supercapacitors(SCs), in particular, are currently drawing lot of interests due to their potential to deliver high power densities in short periods of time with high cyclability and durability [24]. In this sense, the graphitic character, porosity, conductivity or the presence of oxygen functionalities could greatly affect the properties of SCs, providing us with important information about the presence of oxygen functionalities on the surface. The cyclic voltammogram (**Fig.4.5**) of the material in the scan rate range 5-200 mV/s indicated good capacitance behaviour. The single electrode specificcapacitance was determined to be ~64 F/g for the lowest scan rate at which a quasi-rectangular profile was observed **(Table 4.1)**. A low scan rate is believed to allow the electrolyte to penetrate deeper into the pores making greater contact with the internal surface of the electrode material enhancing charge storage capacity [25]. With the sweep rate increasing, the CV traces get tilted implying that the IR drop for electrolyte motion in carbon pores affects the double-layer formation [26].

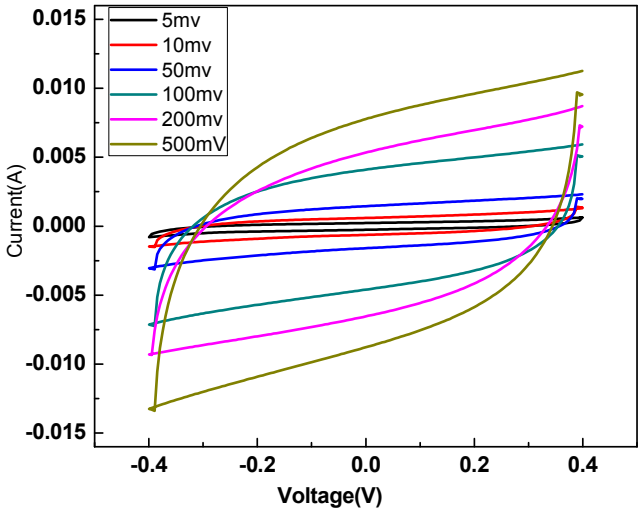

Fig.4.5.CV curves of electrode prepared using CNS at different scan rate (5 - 200 mV/s) in 1N KOH solution

Table 4.1 Specific capacitance at different scan rate

Scan rate (mV/s)	Current (m A)	Total specific capacitance(F/g)	Specific capacitance of a single electrode (F/g)
5	0.37	32.13	64.26
10	0.61	30.72	61.44
50	2.67	26.73	53.46
100	4.29	21.47	42.94
200	5.85	14.64	29.28
500	8.07	8.07	16.14

4.3. Carbon nanocubes from Bean Seeds *(Phaseolus sp.)*

4.3.1.Materials

The *Phaseolus* sp.commonly called beans is an herbaceous annual plant grown worldwide for its edible dry seed or unripe fruit. Being a member of the legume family *Fabaceae*, they acquire nitrogen through an association with rhizobia, a species of nitrogen-fixing bacteria. The seeds (**Fig.4.6**) were collected during winter season from the villages of Hailakandi, Assam, India and were thoroughly washed, sun dried, crushed and used as precursor to synthesize carbon nanocubes. It is pertinent here to mention that the such beans species yielding multi colour variety of seeds**(Fig.4.6(b))** used for the synthesis is a unique agro-product of North East India as this variety, not available in other parts of country.

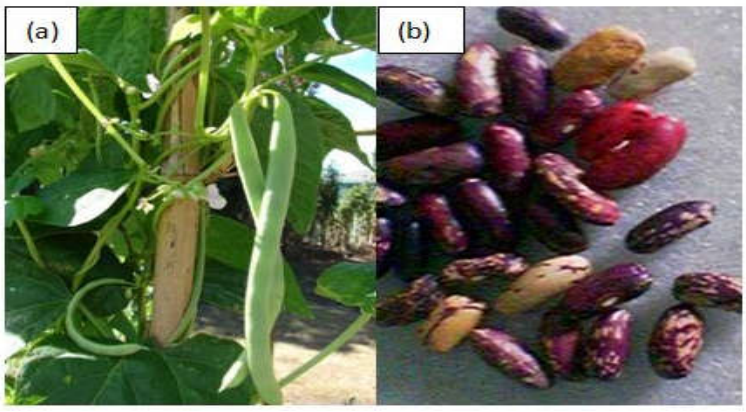

Fig.4.6. Photographs of bean *(Phaseolus* sp.*)* **(a)** plant and **(b)** seeds

4.3.2. Preparation of carbon nanocubes

Carbon nanocubes were obtained by pyrolysis of bean seeds in chemical vapour deposition furnace. The washed, dried and crushed seeds (~10g) were kept in a quartz

boat of CVD chamber and heated to 800^0C at a rate of 7^0C /min for 2 hours under inert condition of argon gas flow at a rate of $6cm^3$/min. The method afforded a black powder that was collected and analysed (yield 2.8 g).

4.3.3. Results and discussion

The synthesized carbon nanocubes black powder is air stable for months and can be dispersed in aqueous and organic solvents (methanol, ethanol) under ultrasonication. The yield of the nanomaterial was found to be around 28% by weight of the initial biomass.

4.3.3.1. Scanning electron microscopy and transmission electron microscopy

The SEM micrographs**(Fig.4.7(a,b))** revealed the presence of uniform monodispersed nanoparticles.

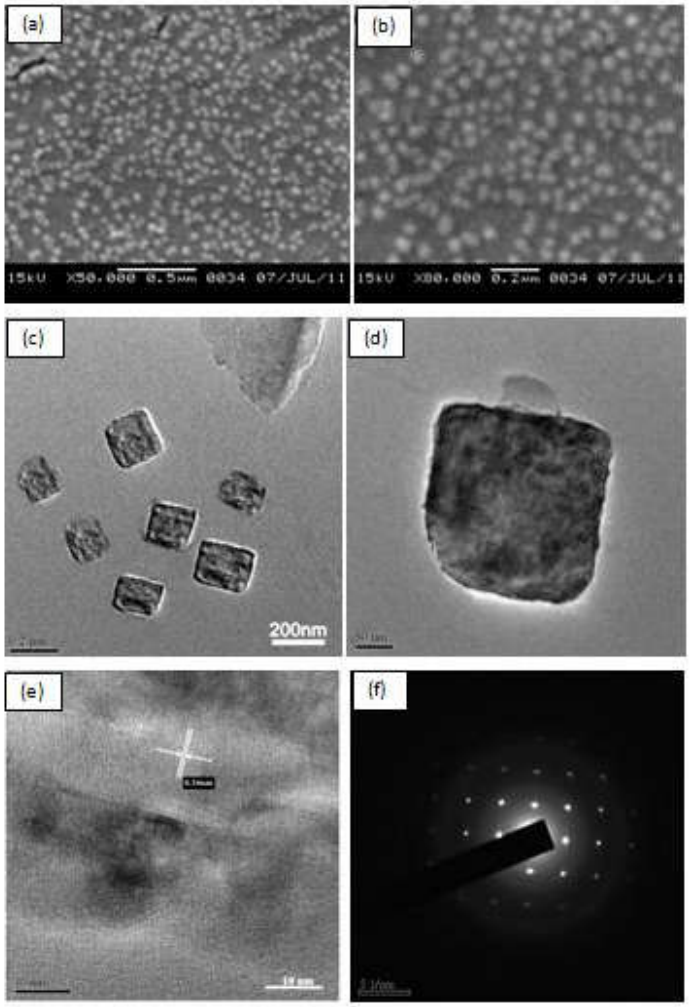

Fig. 4.7. (a) SEM micrograph (b-d) TEM micrographs (e) HRTEM micrograph (f) SAED pattern of the carbon nanocubes obtained from bean seeds

The TEM micrographs **(Fig.4.7 (c,d))** showed the presence of quasi cubic particles in the nano dimension with coarse surface. The size of the particles is ~150nm**.** The HRTEM image showed the lattice fringes between the two adjacent planes to be 0.33nm (**Fig.4.7(e**)) apart which corresponds to the interplanar separation of the (002) plane hexagonal graphitic carbon. Poly-crystallinity of the material was confirmed from the SAED pattern **(Fig. 4.7 (f)).**

It is pertinent herein to mention that the synthesis of carbon nanocubesby laser ablation of graphite is documented in literature [27]. The enhanced photo-luminescent property of these nanocubes is obtained by surface modification with organic polymeric materials or with impurities to impose quantum confinement [27-30]. The present work on the bio-based synthesis of carbon nano-cube significantly simplifies the synthesis of this highly potential material.

4.3.3.2. Powder X-ray diffraction study of carbon nanocubes

The powder X-ray diffraction patternwas recorded for identification of phases exhibited by the synthesized material. The XRD pattern **(Fig.4.8)** showed the presence of a broad major peak centered at ~$26^0$and secondary peaks ~44^0, ~53^0 related to the (002), (101) and (004) planes of hexagonal graphitic carbon respectively. The broad diffraction peaks indicating reduced crystallite size. The average crystallite size for the most intense peak by Debye-Scherrer formula, using a Gaussian fit was found to be 17.8 nm.

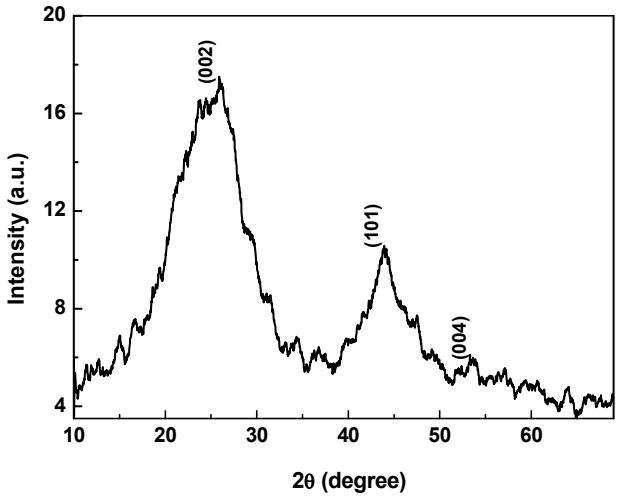

Fig.4.8. PXRD pattern of carbon nanocubes

4.3.3.3. Raman Spectrum of carbon nanocubes

Raman spectra have been recorded to disclose the graphitic ordering of the synthesized nanomaterials. (**Fig.4.9)** shows a representative Raman spectrum with characteristic D and G bands centered at 1330 cm^{-1} and 1589cm^{-1} respectively. The D band is related to the defects and disorder-induced modes and the G band is associated with the vibration of sp^2 bonded carbon atoms in a two dimensional hexagonal lattice [21, 22]. The I_D/I_G ratio is related to graphitic ordering in carbon materials and is found to be 0.8503 showing a high degree of graphitization[21].

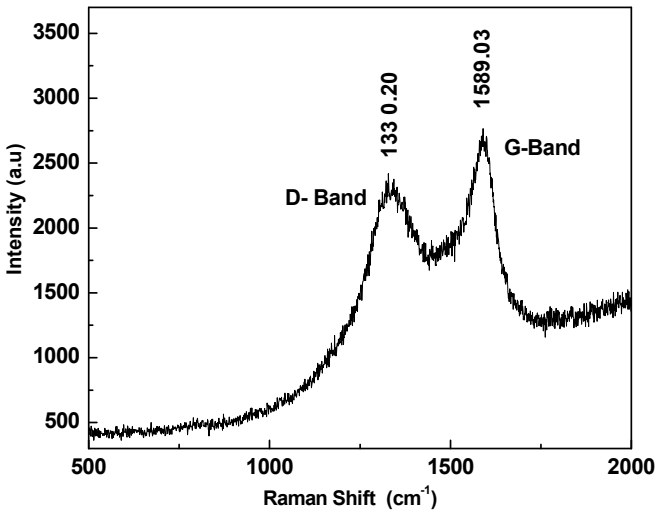

Fig.4.9. Raman spectrum of carbon nanocubes

4.3.3.4.Electrochemical behaviour of as-obtained carbon nanocubes

Carbon nanostructures have attracted much attention in the field of sustainable energy technologies, organic photovoltaics conductive films for solar cells, batteries, super-capacitors, and fuel cells etc. [31-38]. Porous carbon nanostructureswere found to have high specific capacity, cyclic stability, and higher working voltage when used aselectrodes for supercapacitors [39]. Theelectrochemical double layer capacitor operates by adsorbing/desorbing charged ions from an electrolyte onto their highly porous high surface area electrodes. The capacitance at one electrode interface is given by $C=\varepsilon A/4\Pi t$ (where ε is the dielectric constant of the electrical double-layer region, A. The surface-area of the electrode, and t the thickness of the electrical double layer). The combination of high surface area and small charge separation is essential for an extremely high capacitance [39].

In the present work, the two-electrode system is used to evaluate the performance of capacitor cell in 1N KOH electrolyte**.** The Cyclic Voltammograms (CVs) of synthesized material at scan rates of 5 to 500 mV/s exhibited capacitive behaviour with respect to applied voltage of -0.4 to 0.4 V (**Fig.4.10**). CV curve showed a quite rectangular shape at 5 mV/s indicating well developed capacitance properties. Up to the scan rate of 200mV/s, the CV curve shows rectangular shape after that it shows elliptical behaviour. The specific capacitance (Csp) is calculated using the relation,Csp = I/sxW, where W (g) is the total weight of the material used for construction of cell and s (V/s) is the scan rate. Specific capacitanceof a single electrode (Cp) in a capacitor cell is calculated using the expression, Cp= 2 x I/(dv/dt) x w = 2x C_{total}/w. The specific capacitance of the synthesised material at different scan rate is presented in **Table 4.2**

Table4.2 Specific capacitance at different scan rate

Scan rate (mV/s)	**Current (m A)**	**Total specific capacitance (F/g)**	**Specific capacitance of a single electrode (F/g)**
5	0.59	59.65	119.30
20	1.70	42.72	85.44
50	3.74	37.41	74.82
100	4.66	33.33	66.66
200	7.14	17.85	35.70
500	8.76	8.76	17.52

It is observed that scan rate is inversely proportional to specific capacitance**(Table 4.2).**As the scan rate increases, current increases but specific capacitance decreases. It is considered that slowing down the scan rate can allow electrolyte to penetrate into pores more thoroughly and to make greater contact with the internal surface of the electrode material and hence more charge is stored on the surface of electrode and yield a larger measured capacitance that is closer to the intrinsic capacitance [40]. At higher scan rate electrolyte get less time to contact with the complete electrode surface and less charge stored on electrode surface which resultedinto low

capacitance[40, 41]. The specific capacitance determined for a single electrode to be 119.3 F/g at scan rate 5mV/s.

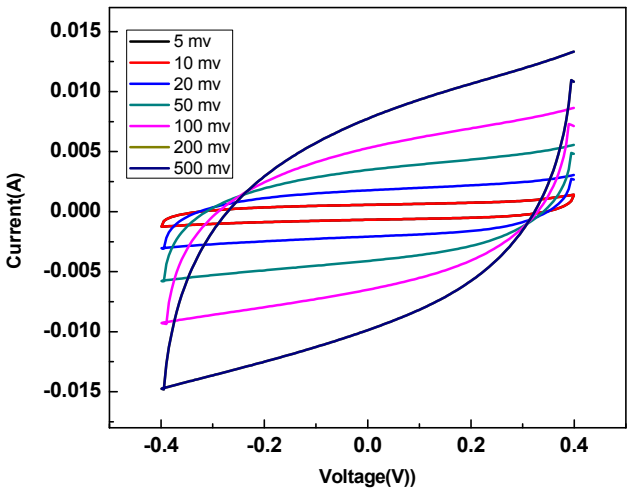

Fig.4.10.CV behaviour of electrode prepared using carbon nanomaterials at different scan rate (5 - 500 mV/s) in 1N KOH solution

Another technique, constant current charge/discharge, was used to evaluate capacitance. (**Fig.4.11)** shows graph of Charge-Discharge cycle (CD) where the slope of the CD curve represents the scan rate of around 20mV/s. During the test, 1 mA was used as the constant current, consistent with the CV measurement.

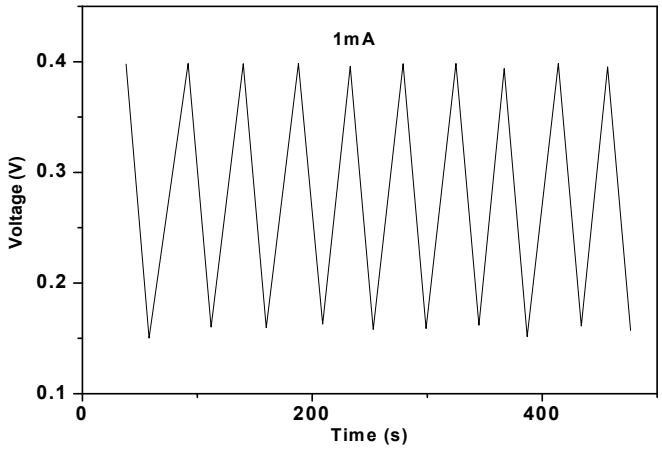

Fig.4.11. Charge-Discharge curves of a capacitor cell made with carbon nanomaterials at current of 1mA

The potential range was kept between -0.4 to 0.4V.The purpose for keeping these parameters constant was to determine the capacitance values from these two methods are comparable. It was found that slope of charging and discharging curve was same. However, the capacitance determined using the CD method at 20mV/s was (42.0 F/g) which was almost same the one obtained with the CV method (42.7 F/g).

4.3.3.5.Antioxidant activity of carbon nanocubes

The potential role of carbon nanostructures as free-radical scavengers is an emerging area ofresearch [42]. The compounds with long conjugated C=C networksincluding graphite and graphene have been proven to be free radical scavengers[43, 44]. No documentary evidence signifying free radical scavenging ability of carbon nanocubeshas been found.The antioxidant activity of as -obtained carbon nanocubes was measured on the basis of the scavenging ability of the stable 1, 1- diphenyl 2-picryl hydrazyl (DPPH) free radical [45]. An amount of 4 mg powdered sample was taken in a test tube and treated with 3 mL, 100 μM methanolic solution of DPPH. The aforementioned procedure was followed to ascertain time dependent DPPH scavenging at periodic interval of 15, 30, 45 and 60 minutes.The percentage scavenging was calculated using the formula:

$$\text{DPPH scavenging (\%)} = [(A_c - A_s)/A_c] \times 100$$

where A_C and A_S are absorbances of the control DPPH and DPPH with the nanocomposites at 517 nm respectively. For evaluating SC-50 (the amount of samples required to scavenge 50% of DPPH), a similar procedure was adopted for 2, 4, 6, 8, 10, 15 and 20 mg of the nanomaterial and absorbances recorded after 30 minutes.

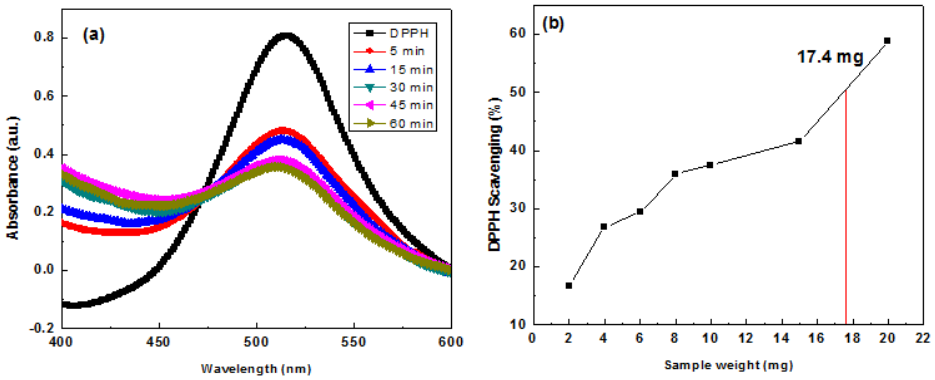

Fig.4.12. (a) Time dependent DPPH free radical scavenging **(b)** DPPH scavenging (%) at different weight of as prepared nanocubes.

It is evident from the **Fig.4.12.(a)**that nanomaterials driven steady decrease of DPPH absorbance at 517 nm with time due to the scavenging of free radical [45-47]. It is apparent from the **Fig.4.12** that after 60 minutes more than60% of the DPPH got scavenged for 20mg of the nanomaterials. The SC-50 value was ascertained graphically (**Fig.4.12 (b))** and was foundto be 17.4 mg.

4. 4. Carbon nanoparticles from castor oil seed and castor seed coat *(Ricinus communis)*

4.4.1 Materials

Castor beans, the seeds of *Ricinus communis*, a member of the spurge family (Euphorbiaceae), are among the most infamous seeds in the world.Besides being used and for culinary purposes. The seeds (**Fig.4.13 (b)**) were collected from villages of Hailakandi, Assam, India and the seed coats **(Fig.4.13(c))** were scrabbled up, thoroughly washed and sun dried. The dry biomasses were used as precursors to synthesize nanomaterials.

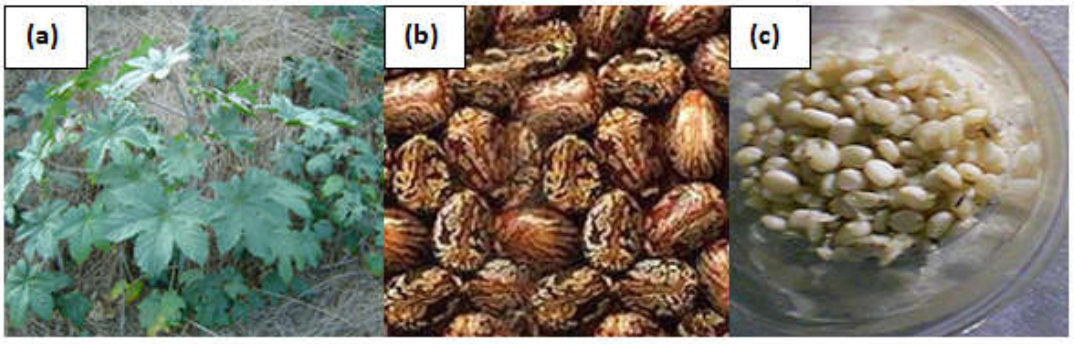

Fig.4.13. Photographs of**(a)**castor oil plant **(b, c)**castor oil seeds

4.4.2Synthesis of carbon nanomaterials

(a) Carbon nanoparticles from seed coat: A quartz boat loaded with the dried and crushed seed coat (10 g) inserted in a horizontal quartz tube is placed in the furnace. The tube was initially flushed with argon gas to eliminate air from the tube. The gas was then purged at a flow rate of 6cm^3/min. The furnace was heated to 800^{0}C at a rate of 7^{0}C min^{-1} for 2 hours to complete the process of pyrolysis. The system was then allowed to cool to room temperature under inert condition and the black powdered materials was collected from the quartz boat and analyzed (yield 2.4 g).

(a) Carbon nanoparticles from seed: Approx.10 g of the castor seed was taken in a quartz boat which was placed inside a quartz tube of the CVD chamber. The carrier gas argon was allowed to flow into the quartz tube with a fixed flow rate of 6 ml/min. The flow of carrier gas was maintained throughout the experiment. After 15 min of flow, furnace was switched on to reach the desired temperature 800^0C. After the completion of pyrolysis, furnace was switched off and carbon nanomaterial formed inside the quartz tube was collected and analysed 'as obtained'. The yield was recorded to be 2.9g.

4.4.3. Results and discussion

The as-obtained carbon nanomaterial black powder from both seed and seed coat of castor are found to be air stable for months and can be dispersed in aqueous and organic solvents (methanol, ethanol) under ultrasonication. The yields of the nanomaterials were found to be around 30% and 25% by weight of the initial biomass of castor oil seed and seed coat respectively.

4.4.3.1. Scanning electron microscopy

The scanning electron microscopy was used to study the surface morphology of the 'as obtained' materials from both castor oil seed and seed coat. The SEM micrographs **(Fig.4.14 (a, b))** of the materials obtained from castor oil seed showed the presence of non-uniform porous blocks of larger dimension (200μm). Small particles of irregular shape and size were found to be scattered over the surface of the blocks. However, the SEM micrographs**(Fig.4.14 (c, d))** of materials from seed coat revealed nearly spherical monodispersed particles of average size 20-25 nm.Itis pertinent here to mention that thecastor oil seed on pyrolysis at 850^0C in hydrogen environment resulted weived with rope like structures [48,49].

4.4.3.2. Transmission electron microscopy

TEM micrographs (**Fig.4.15**) of the materials obtained from castor oil seed coat revealed the presence of agglomerated quasi-spherical particles. The particle size is found to be in the range of 15-25 nm. The SAED pattern is indicative of polycrystalline nature.

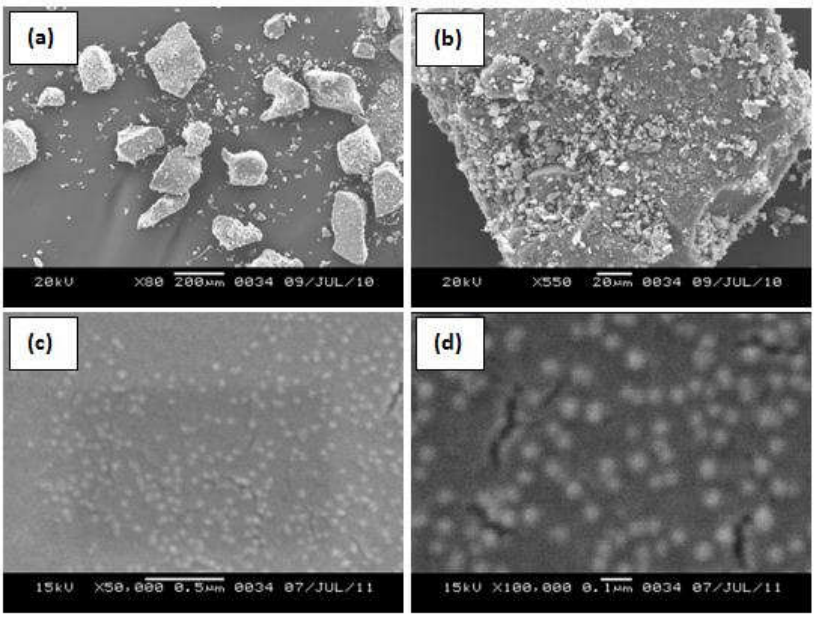

Fig.4.14. SEM Micrographs of **(a, b)** carbon nanomaterials from castor oil seeds and **(c, d)** carbon nanoparticles from castor oil seed coat

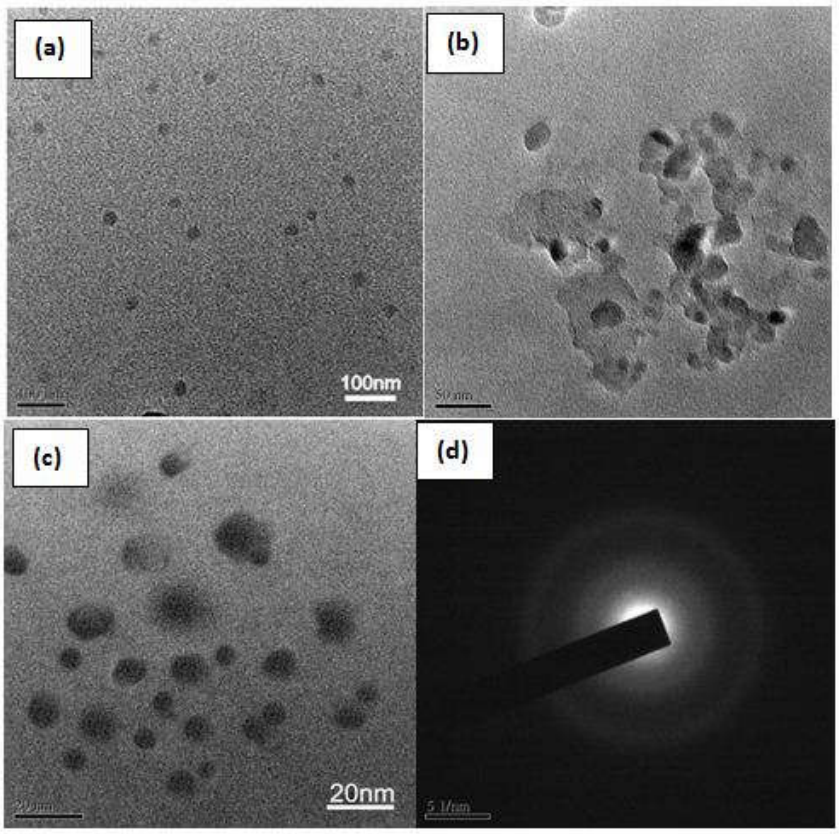

Fig.4.15. (a-c) TEM micrograph **(d)**SAED pattern ofcarbon nanoparticles fromcastor oil seed coat

4.4.3.3. XRD analysis of carbon nanoparticles from castor seed coat

The XRD pattern **(Fig.4.16)** exhibited the presence of a major peak centered at ~26^0 related to the (002) and other secondary peaks corresponding to (002), (100), (101), (102) (004) and (103) reflections corresponds to hexagonal graphitic carbon.The broad nature of the diffraction peaks indicating the reduced crystallite size. The average crystallite size for the most intense peak by Debye-Scherrer equation using a Gaussian fit was found to be 15.3nm. The interlayer spacing (d_{002} = 0.34nm) found by XRD is characteristic of graphitic carbon.

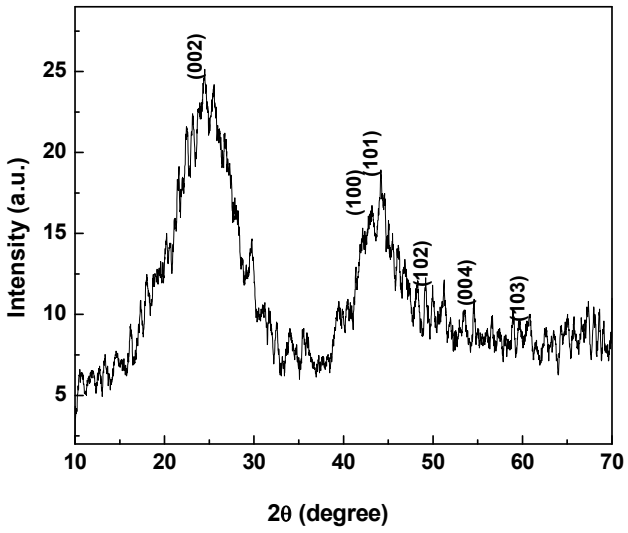

Fig.4.16.XRD pattern of carbon nanoparticles from castor oil seed coat

4.4.3.4. Raman studyofcarbon nanoparticles from castor oil seed coat

Raman spectrum(**Fig.4.17)** associated to carbon materials presents two main peaks at Raman shifts of ca. 1330.20 and 1589.03 cm^{-1}, commonly denoted as D- and G-bands respectively. The former is usually associated with the impurities that destroy the graphitic symmetry, while the latter represents the splitting of the E_2g stretching mode for the graphite [21]. The ratio of relative intensities of D- and G-bands (I_D/I_G) is commonly used as an index to assess graphitic character [21]. The intensity ratio I_D/I_G= 0.88 (< 1) higher degree of graphitization [21, 22].

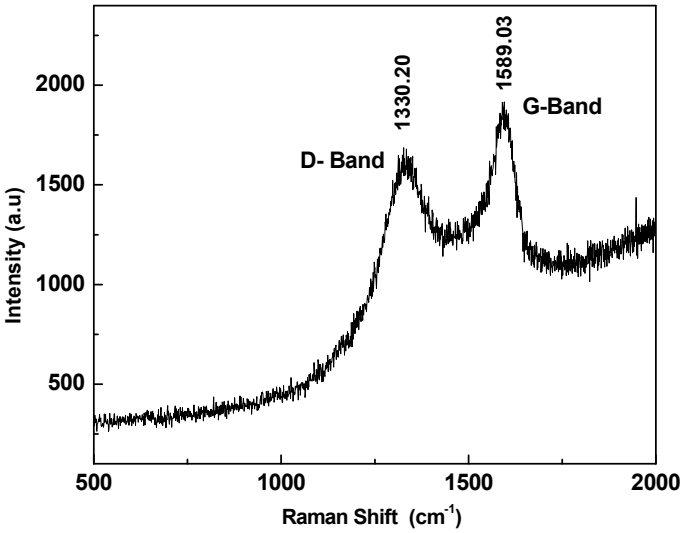

Fig.4.17. Raman spectrum of carbon nanoparticles from castor seed coat

4.4.3.5. Electrochemical behaviour of carbon nanoparticles from castor oil seed coat

Supercapacitors are energy storage devices that can supply extremely high but transient power output[39]. They are being both utilized and considered for numerous power source applications, such as auxiliary power sources for hybrid electric vehicles and short term power sources for mobile electronic devices [50-52]. Recently, electrochemically active carbonaceous materials have attracted much attention as materials for supercapacitor.Thus the carbon nanoparticles from castor seed coat were studied to measure the electrochemical performance through cyclic voltammetry (CV) and Galvanostatic charge/ discharge (CD).

The Cyclic voltammograms of as obtained material at scan rates of 5 to 500 mV/s exhibited capacitive behaviour with respect to applied voltage of -0.4 to 0.4 V **(Fig.4.18 (a)).** It can be noted that the shape of CV for carbon nanoparticles is very close to a rectangle at 5mV/s suggesting that the capacitance of CNPmainly contributed by electric double-layer capacitance. The specific capacitance of the synthesized material at different scan rate is presented in **Table 4.3.**

Table 4.3 Specific capacitance at different scan ratefor 0.002 g of CNPs

Scan rate (mV/sec)	Current (mA)	Total specific capacitance (F/g)	Specific capacitance of a single electrode(F/g)
5	0.75	75.08	150.16
10	1.11	55.89	111.78
20	2.08	52.20	104.40
50	2.84	28.48	56.96
100	5.81	26.08	52.16
200	8.76	21.91	43.82
500	13.12	13.12	26.24

It is observed that the specific capacitance decreased with the increase of scan rates from 5 to 500mVs^{-1}**(Table4.3)**.At a high scan rate (500mVs^{-1}), diffusion of electrolyte ions was limited due to the time constraint and only the outer active surface was utilized for charge storage. The maximum specific capacitance of the CNP was 150 F g $^{-1}$ at 5mVs^{-1} and 26.24 F g^{-1} at 500mVs^{-1}.

Constant current or charge/discharge**(Fig.4.18 (b))** was also used to evaluate capacitance of the synthesized CNPs.Constant current or galvanostatic charge/discharge is in principle the same technique as cyclic voltammetry but with fixed current and charge/discharge time.During the test, 1mA was used as the constant current, consistent with the CV measurement. The potential range was kept between -0.4 to 0.4V. The purpose for keeping these parameters constant was to determine the capacitance values from these two methods are comparable. It was found that slope of charging and discharging curve was same. However, the capacitance determined using the CD method at 20mV/s was 54.29 F/g which was almost same the one obtained with the CV method (52.20 F/g). It is worth mentioning that the present study showed a remarkable increase in specific capacitance value (~75 F/g) of carbon nanostructures obtained from castor oil seed coat than that reported by other researchers (~44 F/g) from castor oil seeds[19].

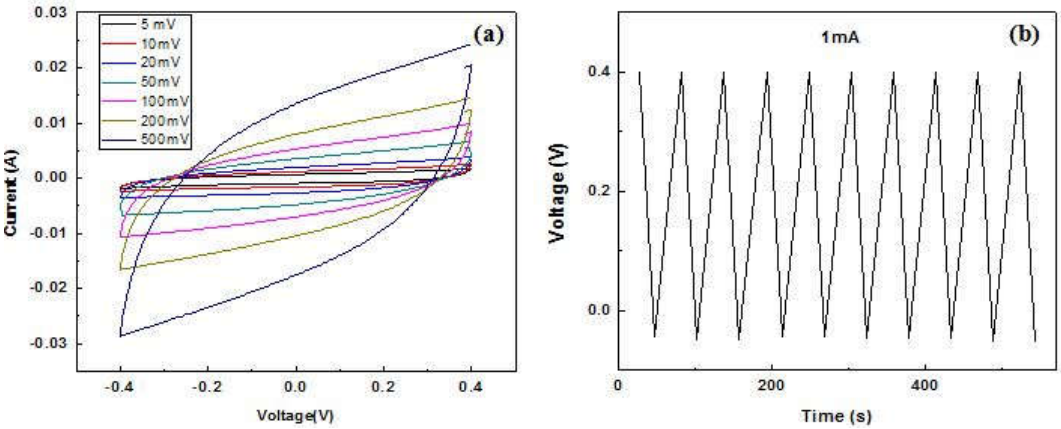

Fig.4.18. (a)CV curve at different scan rate (5 - 500 mV/s) in 1N KOH solution**(b)**CD curve at current of 1 mA of a capacitor made with as prepared carbon nanoparticles

4.5.Carbon nanoparticles from *Brassica juncea* (lai) seed

4.5.1. Materials

*Brassica juncea*is a species of mustard plant commonly called Lai.The leaves, the seeds, and the stem of this mustard variety are edible. These are grown as greens and for the production of oilseed. Seeds of leafy vegetable *Brassica juncea***(Fig.4.19)**were collected from Hailakandi, Assam, India used as carbon precursors for the synthesis of the carbon nanoparticles.

Fig.4.19. Photographs of **(a)***Brassicajuncea*leaves and **(b)***Brassica juncea seeds*

4.5.2. Preparation of carbon nanoparticles(CNP)

Carbon nanoparticles were produced fromseeds of *Brassica juncea* by pyrolysis in a CVD furnace. A quartz boat loaded with the dried seeds (~10 g) inserted in a horizontal quartz tube is placed in the furnace. The tube was initially flushed with argon gas to eliminate air from the tube. The gas was then purged at a flow rate of

6cm^3/min. The furnace was heated to 800 ^{0}C at a rate of 7 ^{0}C min^{-1} for 2 hours to complete the process of pyrolysis. The system was then allowed to cool to room temperature under inert condition and the black powdered materials was collected from the quartz boat and analyzed (yield 2.4 g).

4.5.3. Results and discussion

The 'as obtained' carbon nanoparticles black powder is air stable for months and can be dispersed in aqueous and organic solvents (methanol, ethanol) under ultrasonication. The yield of the material was recorded to be around 25% by weight of initial biomass. Tap density of the material was calculated to be 0.27gcm^{-3}.

4.5.3.1.Scanning electron microscopy

The SEM micrograph **(Fig.4.20 (a))**of the synthesised carbon nanoparticles showed that the particles were monodispersed with no agglomeration and irregular in shape having sizes in the range 20-30nm.

4.5.3.2. Transmission electron microscopy

The TEM micrographs of the as obtained materials**(Fig.4.20 (b-d))** revealed the presence of quasi spherical particles with diameter in the range of 20 -25nm. The average crystallite size calculated from Raman spectrum is in close agreement with that obtained from TEM image. From high-resolution TEM image, the lattice fringes **(Fig.4.20 (e))** were observed at an interplanar distance of 0.33 nm which correspond to (002) plane of graphitic carbon. The SAED pattern revealed the polycrystalline nature of the material **(Fig.4.20 (f)).**

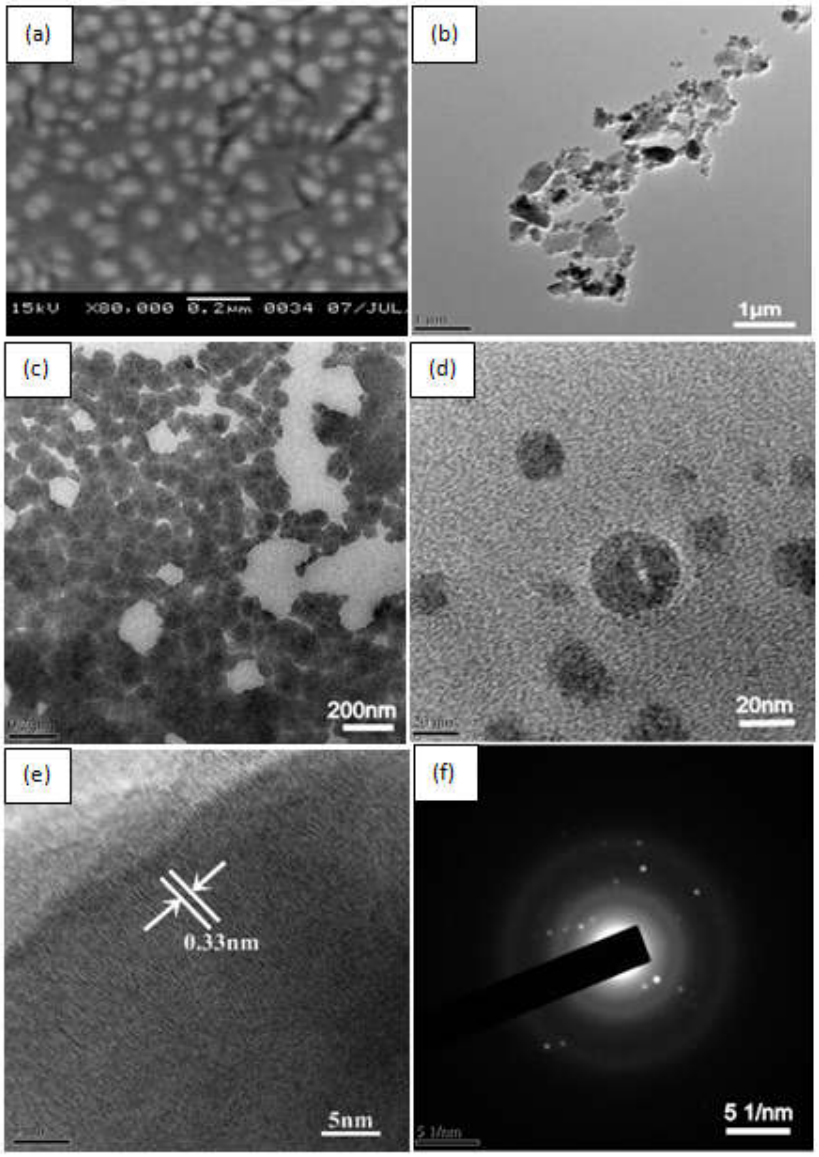

Fig.4.20. (a) SEM micrograph **(b-d)** TEM micrographs**(e)**HRTEM micrograph **(f)**SAED pattern of the materials obtained from *Brassica juncea* seed

4.5.3.3. Powder X-ray diffraction study

The powder XRD spectrum of the as-obtained carbon nanoparticles**(Fig.4.21)** showed three major Bragg peaks at $2\theta = 25.58^0$, 43.51^0 and 50.96^0 corresponding to the (002), (101) and (102) planes, respectively of hexagonal graphitic carbon possessing $P6_3/mmc$ space group (JCPDS Card No. 23-0064). The broad nature of these peaks suggests a lesser long range structural order. Interlayer spacing (d=0.33nm) obtained from TEM and a similar value extracted from Bragg's equation evidences a rather high degree of graphitic character of carbon nanoparticles.

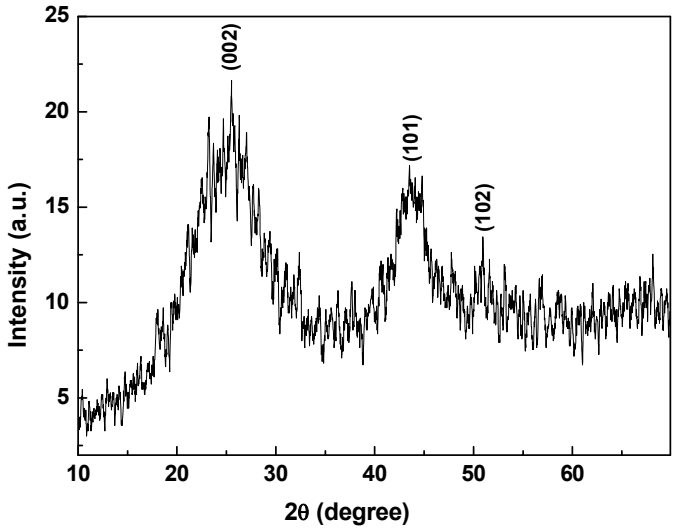

Fig.4.21.XRD pattern of carbon nanoparticles obtained from *Brassica juncea*seeds

4.5.3.4. Raman studyof carbon nanoparticles

Raman Spectrum **(Fig.4.22)** of the CNP exhibited characteristic first order D- and G-bands of graphitic carbon at 1330.20 cm^{-1} and 1596.25 cm^{-1}, respectively. The G band corresponds to the tangential stretching (E_{2g}) mode of the highly oriented pyrolytic graphite [21]. The D-peak assigned to A_{1g} mode originates from the disorder in the sp^2-hybridized carbon and indicates a lattice distortion in the graphitic carbon [22]. The intensity ratio (I_D/I_G) was found to be 0.9198 (<1) indicating a higher degree of graphitization in the material [21].

The crystallite size (L)of graphitic samples can be measured using the (I_D/I_G) ratio fromthe expression,

$$L\ (nm) = 560/E_l^4\ (I_D/I_G)^{-1},$$

where E_l(=2.41eV) is the excitation laser energy. Considering the laser line wavelength λ_l(=514.5 nm)in nanometer, the equation can be rewritten as,

$$L(nm) = (2.4x10^{-10})\ \lambda_l^4\ (I_D/I_G)^{-1},$$

the crystallite size is calculated to be 18.28nm. The specific surface area is calculated by Sauter formula to be 573.5m^2/g.

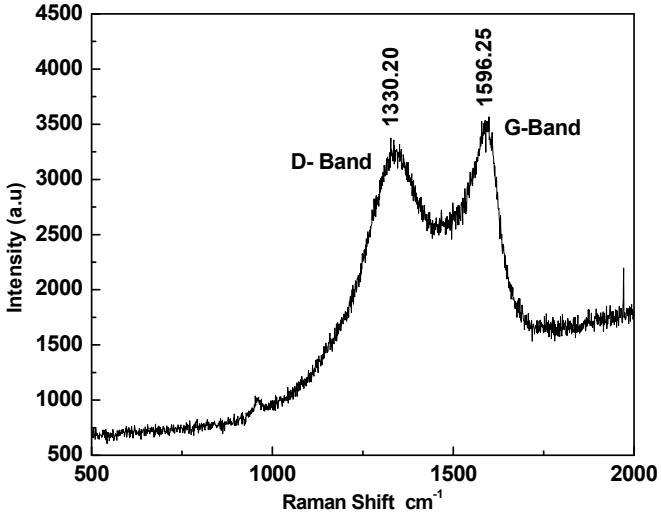

Fig.4.22. Raman spectrumof carbon nanoparticles obtained from*Brassica juncea*seeds

4.6. Carbon nanoparticles from *Amaranthus spinosus* (denga) seed

4.6.1. Materials

Amaranthus spinosus, locally called denga**(Fig.4.23)**, is a cosmopolitan species in the botanical family Amaranthaceae and is commonly known as spiny amaranth. Like several related species, *Amaranthus spinosus* is a valued food plant in north-east India. The seeds of *Amaranthus spinosus* were collected from Hailakandi, Assam, India and after proper washing and drying used as precursor for carbon nanoparticles.

Fig.4.23. Photographs of **(a)***Amaranthus spinosus* plant **(b)***Amaranthus spinosus*seeds

4.6.2. Synthesis of carbon nanoparticles(CNP)

Carbon nanoparticles were produced from washed and dried seeds of *Amaranthus spinosus* by pyrolysis in a CVD furnace. A quartz boat loaded with the seeds (~10 g) inserted in a horizontal quartz tube was placed in the furnace. The tube was initially flushed with argon gas in order to eliminate air from the tube and then purged at a flow rate of $6cm^3$/min. The furnace was heated to 800^0C at a rate of 7^0C per minute for 2 hours to complete the process of pyrolysis. The system was then allowed to cool to room temperature under inert condition and the black powder so formed were collected from the quartz boat and analyzed as obtained (yield 2.8 g).

4.6.3. Results and discussion

The 'as obtained'black powder is air stable for months and can be dispersed in aqueous and organic solvents (methanol, ethanol) under ultrasonication. The yield of the material was recorded to be around 30% by weight of initial biomass.

4.6.3.1. Scanning electron microscopy and transmission electron microscopy

SEM micrograph **(Fig.4.24)** of the as obtained materialsevoked the presence of monodispersed nearly spherical particles of diameter in the range 20-25 nm.

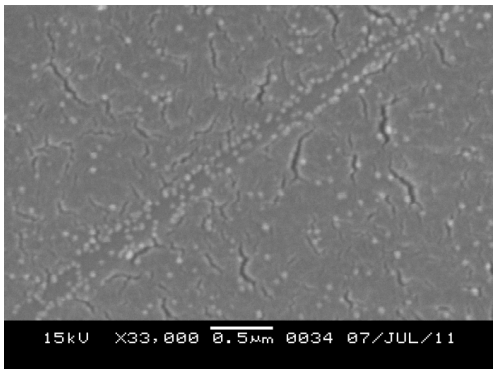

Fig.4.24. SEM micrograph of the nanoparticles obtained from *Amaranthus spinosus*seed

The TEM micrographs **(Fig.4.25. (a,b))** revealed the presence of quasi-spherical nanoparticles and have sizes in the range 20-25 nm. High-resolution TEM image indicated highly crystalline nature of the nanoparticles. From HRTEMimage **(Fig.4.25. (c))**, the lattice fringes were observed to be at interplanar distance of 0.33 nm that corresponds to (002) plane of graphitic carbon. The selected area electron

diffraction (SAED) pattern **(Fig.4.25. (d))**showed concentric rings that are characteristic of graphitic carbon indicating polycrystalline nature of the material.

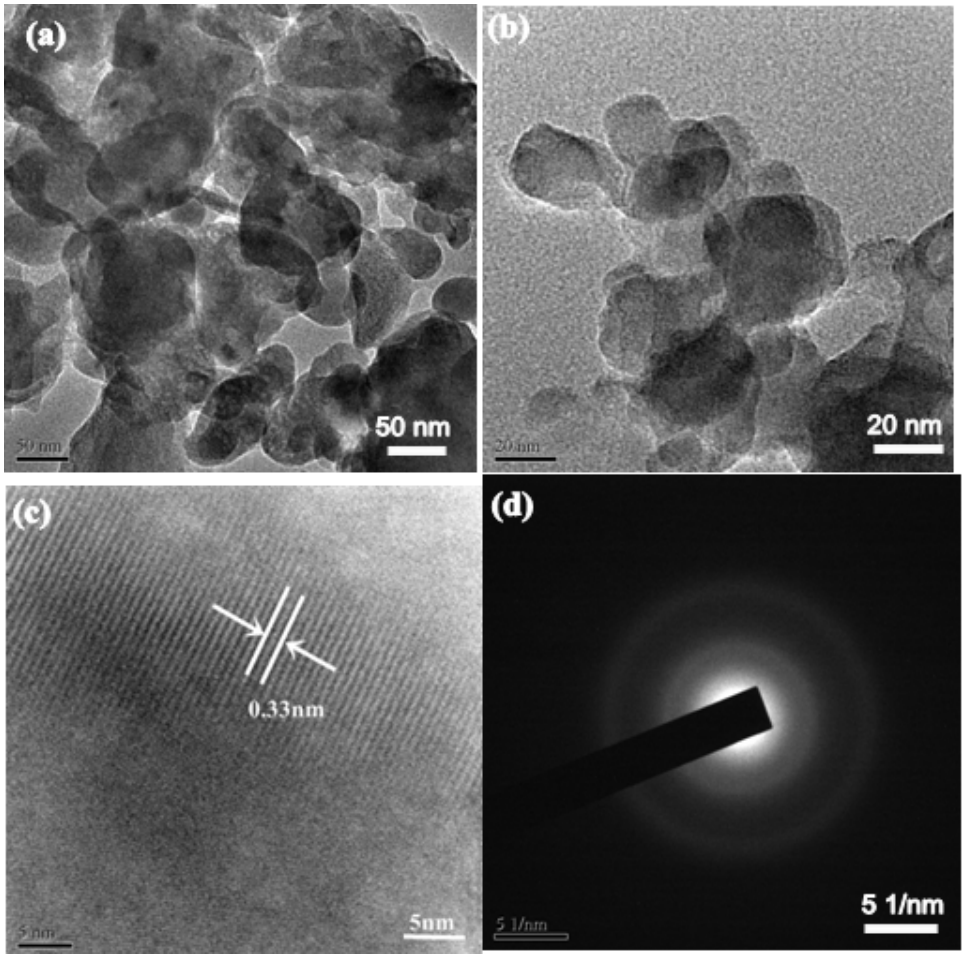

Fig.4.25. (a,b)TEM Micrographs **(c)** HRTEM micrograph **(d)**SAED patternof the carbon nanoparticle obtained from *Amaranthus spinosus*seed

4.6.3.2. Powder X-ray diffraction study of carbon nanoparticles

The powder XRD pattern **(Fig.4.26)** of the as-obtained carbon nanoparticles showed two major Bragg peaks at $2\theta = 26.50^0$ and 43.18^0 along with shoulder peaks at 51.18^0, 55.81^0 and 60.01^0 corresponding to the (002), (101), (102), (004) and (103) planes, respectively of hexagonal graphitic carbon possessing $P6_3/mmc$ space group (JCPDS Card No. 23-0064). The broad nature of these peaks suggests a lesser long range structural order. Interlayer spacing (d=0.33nm) obtained from TEM and a similar value extracted from Bragg's equation evidences a rather high degree of graphitic character of material.

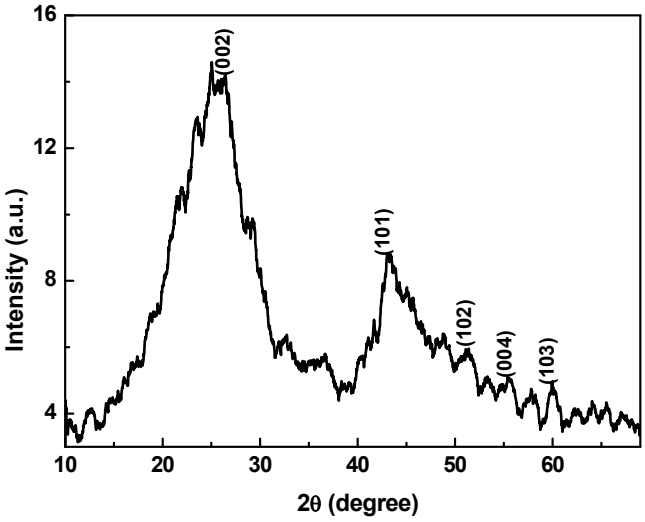

Fig.4.26. XRD spectra of the particle obtained from *Amaranthus spinosus*seed

4.7. Carbon nanoparticles from sandalwood (*Santalum*sp.)seed

4.7.1. Materials

Sandalwood is the name of a class of woods from trees in the genus *Santalum*. The woods are heavy, yellow, and fine-grained, and unlike many other aromatic woods, they retain their fragrance for decades. Both the wood and the oil produce a distinctive fragrance that has been highly valued for centuries. Apart from its fragrance, sandalwood is also used for its many health benefits and therapeutic uses. The sandalwood seeds **(Fig.4.27)**were collected from Hailakandi, Assam, India and thoroughly washed, sun dried, crushed and used as precursor for the synthesis of nanoparticles.

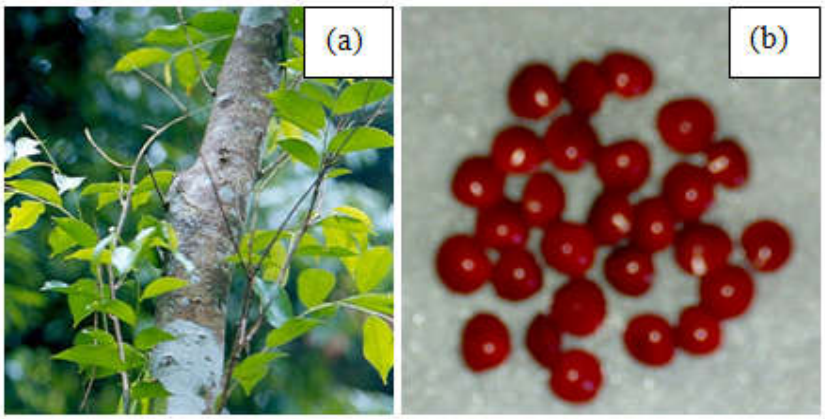

Fig.4.27. Photographs of **(a)** sandalwood tree and **(b)** sandalwood seeds

4.7.2. Synthesis of carbon nanoparticles

Quasi spherical carbon nanoparticles were produced from the dried and crushed seeds ofsandalwoodby pyrolysis in a CVD furnace. A quartz boat loaded with the precursor (10 g) inserted in a horizontal quartz tube was placed in the furnace. The tube was initially flushed with argon gas in order to eliminate air from the tube and then purged at a flow rate of $6cm^3$/min. The furnace was heated to 800^0C at a rate of 7^0C per minute for 2 hours to complete the process of pyrolysis. The system was then allowed to cool to room temperature under inert condition and the black powder so formed were taken out from the quartz boat and analyzed as obtained (yield 3.2 g).

4.7.3.Results and discussion

The 'as obtained' carbon nanoparticles black powder is air stable for months and can be dispersed in aqueous and organic solvents (methanol, ethanol) under ultrasonication. The yield of the material was recorded to be around 30% by weight of initial biomass.

4.7.3.1 Scanning electron microscopy

The scanning electron microscopy is used to investigate the morphology the as obtained materials. The SEM micrographs **(Fig.4.28)** revealed evenly dispersed uniform nanospheres of diameter in the range 50-60nm.

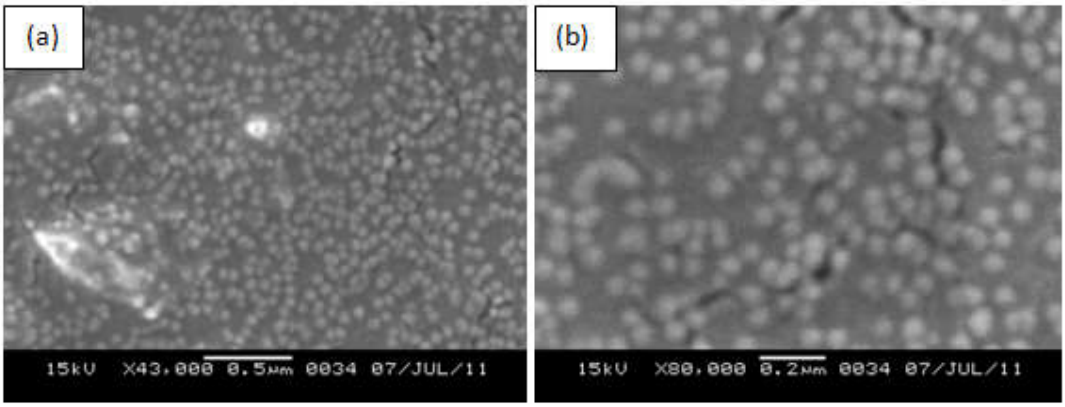

Fig.4.28. (a,b) SEM micrographsof the particles obtained from sandalwood seed

4.7.3.2. Transmission electron microscopy

Transmission electron microscopy is used to investigate the internal morphology of the as obtained materials. The TEM micrographs **(Fig.4.29 (a,b))** revealed the

presence of carbon nanoparticles of diameter in the range 8-14 nm. From HRTEM image, the lattice fringes **(Fig.4.29(c))** were observed at an interplanar distance of 0.33 nm which correspond to (002) plane of graphitic carbon. The SAED pattern **(Fig.4.29 (d))** attested the polycrystalline nature of the material.

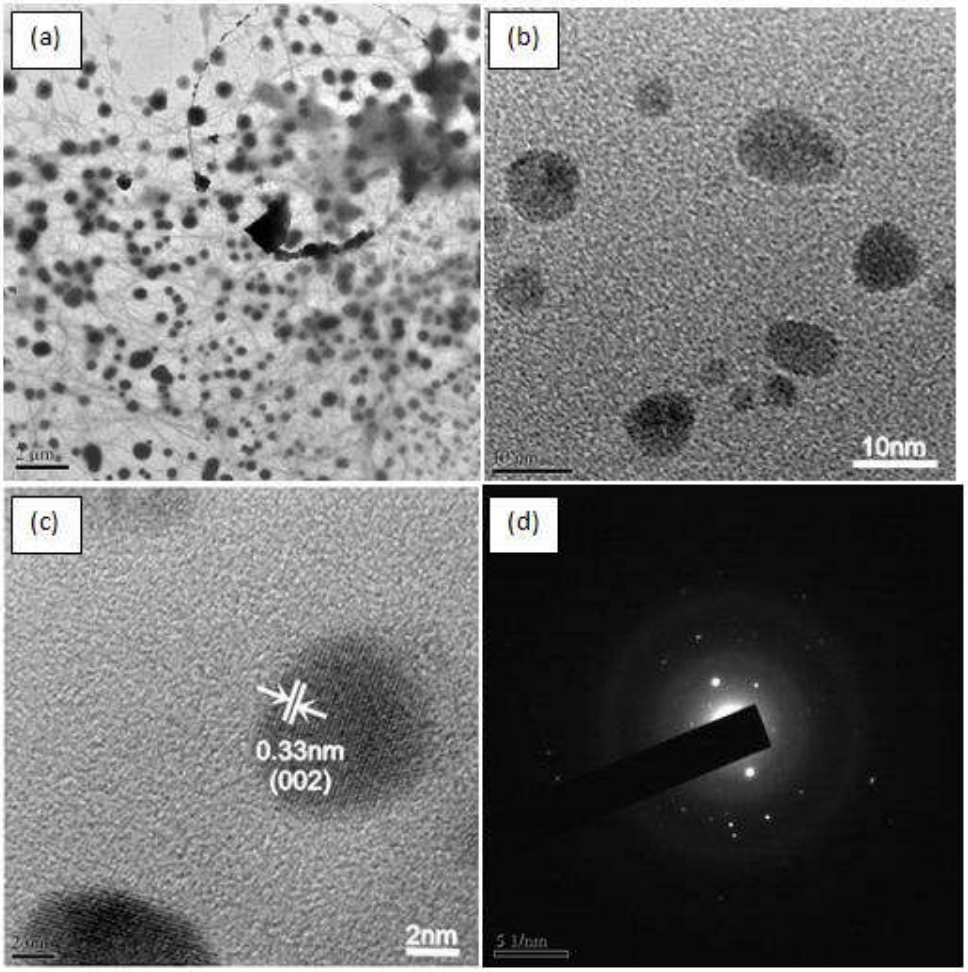

Fig.4.29.(a,b) TEM micrographs **(c)**HRTEM micrograph **(d)**SAED pattern of the particles obtained from sandalwood seed

4.7.3.3. Powder X-ray diffraction analysis of carbon nanoparticles

The powder XRD pattern **(Fig.4.30)** of the as-obtained carbon nanoparticles showed diffraction peaks which indexed to the hexagonal graphitic carbon (space group $P6_3/mmc$, JCPDS Card No. 23-0064). Three major Bragg peaks at 2θ = 26.0^0, 42.0^0 and 44.7^0 along with secondary peaks at 51.1^0, 56.0^0 and 59.8^0 corresponding to the (002), (100), (101), (102), (004) and (103) planes of graphite. The broad nature of the peak suggests lesser long range structural order. Interlayer spacing (d_{002}=0.33nm)

extracted from XRDpattern is in close agreement with that obtained from HRTEM study.

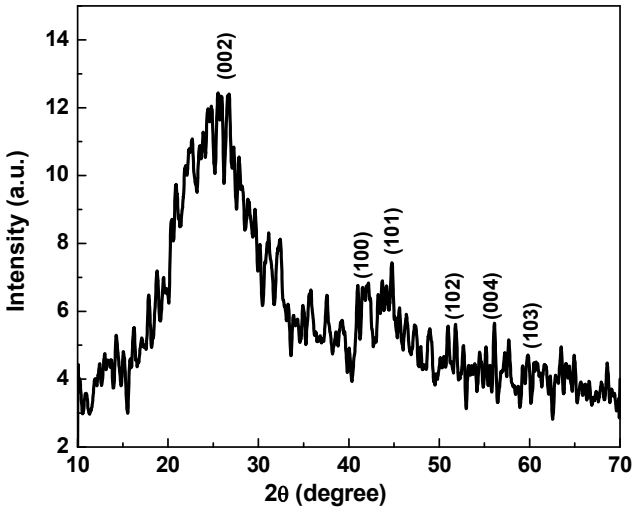

Fig.4.30. XRD pattern of the particles obtained from sandalwood seed

4.8. Carbon nano particles from kanchan (*Bauhinia acuminata*) seed

4.8.1. Materials

Bauhinia acuminata is a species of flowering shrub native to tropical southeastern Asiaand locally known as kanchan**(Fig.4.31)**. It is very popular ornamental flowering tree usually grows two to three meter tall. The leaves are bilobed, shaped like a camel's hoof print. Kanchan is a medicinal tree and used in India from time immemorial of treatment of diseases like leprosy, scrofula, ulcers and other skin diseases. The flowers are of two varieties, purple and white. The seed of white variety is collected for the experiment. The seeds were collected from Hailakandi, Assam, India and after proper washing and drying used as precursor for carbon nanoparticles.

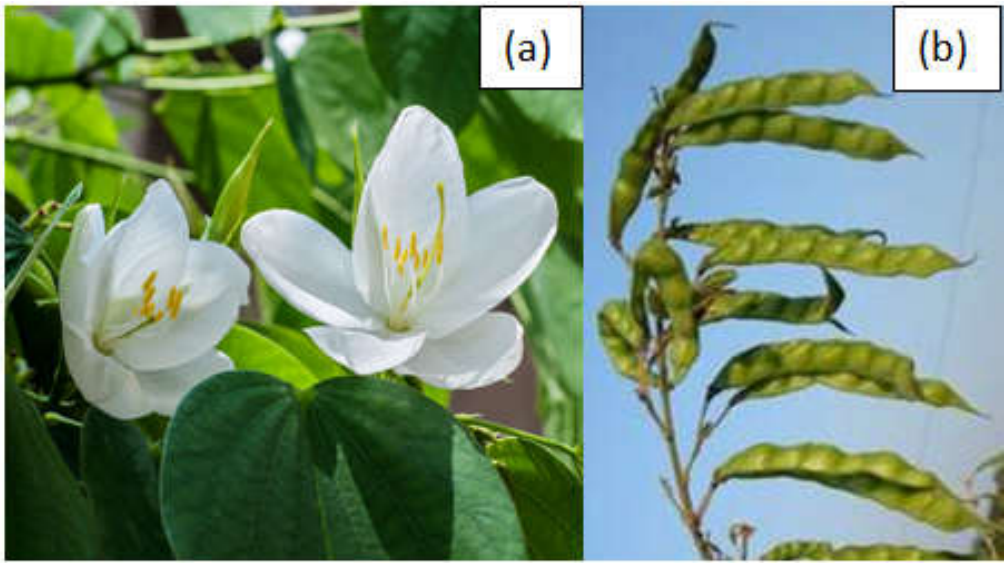

Fig.4.31. Photographs of **(a)** kanchan flower and **(a)** kanchan seeds

4.8.2. Synthesis of carbon nanoparticles (CNP)

Carbon nanoparticles were produced from matured kanchan flower seed (*Bauhinia acuminata*) by pyrolysis in a CVD furnace. The dried biomass (~10g) taken in a quartz tube was heated to 800^0C in a chemical vapour deposition furnace at a rate of 7^0C /min for 2 hours under argon gas flow rate of $6cm^3$/min to afford a black powder. The yield was recorded to be 2.8g.

4.8.3. Result and discussion

The 'as obtained' carbon nanoparticles black powder is air stable for months and can be dispersed in aqueous and organic solvents (methanol, ethanol) under ultrasonication. The yield of the material was recorded to be around 30% by weight of initial biomass.

4.8.3.1. Scanning electron microscopy and transmission electron microscopy

The scanningelectron microscopy and transmission electron microscopy is used to investigate the morphology the as obtained materials. The SEM micrograph **(Fig.4.32(a))** revealed that the nanoparticles are well dispersed with no agglomeration. The particles are quasi spherical and have sizes about 20-30nm. The TEM micrographs validatedthe non-agglomerated quasi spherical particles of size ~30 nm **(Fig.4.32 (b,c)).**The SAED pattern **(Fig.4.32 (d))**showed diffused rings that areindicative of polycrystalline nature of the particles.

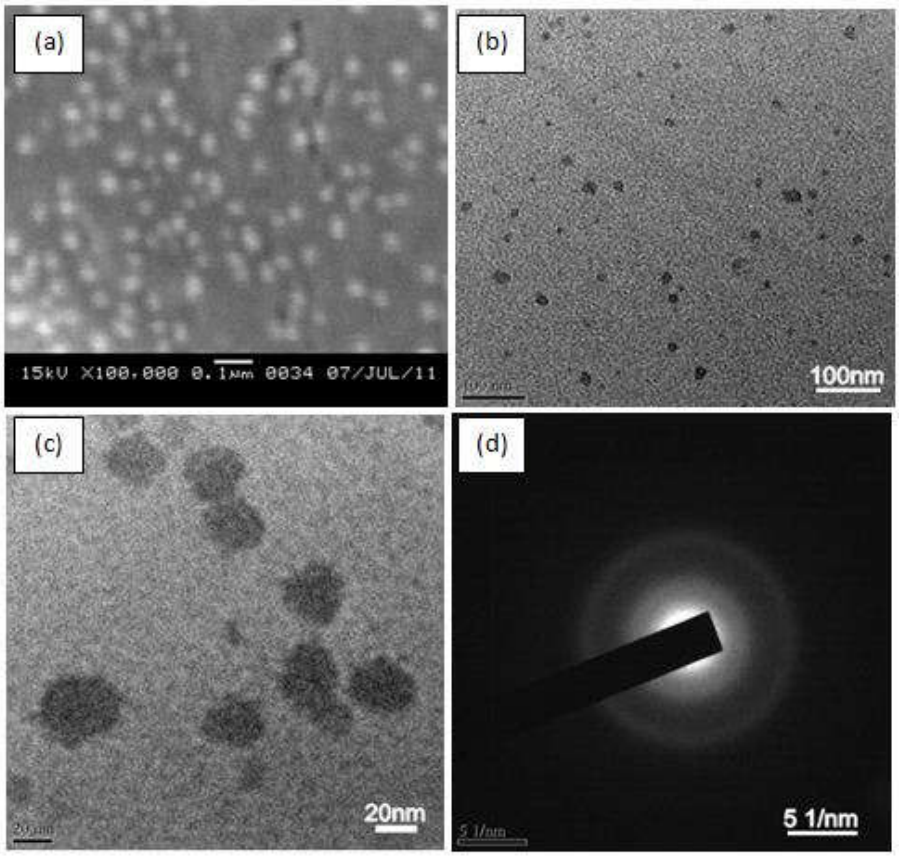

Fig.4.32. (a)SEM micrograph **(b,c)**TEM micrographs**(d)**SAED of the particles obtained from kanchan flower seed

4.8.3.2. Powder X-ray diffraction study and Raman study

The powder X-ray diffractionpattern was recorded for identification of phases exhibited by the synthesised material. The XRD pattern **(Fig.4.33(a))** showed major Bragg peaks at 2θ = 24.8^0, 44.13^0 and 55.64^0 corresponding to the (002), (101) and (004) planes of hexagonal graphitic carbon.The common broadness of the peaks in the XRD peak indicates a low range in the structural order. The interlayer spacing d_{002} of the synthesized carbon nanoparticles using Bragg's equation is 0.35nmwith a low deviation for the ideal d_{002} space (0.34 nm) in a graphitic structure (JCPDS-ICDD Card No. 41-1487). This value is indicative of a relatively well-organized carbon structure.

Together with XRD, Raman spectroscopy provides very useful information on carbon structural order. The Raman spectrum **(Fig.4.33(b))** of the CNP exhibited characteristic first order D- and G-bands of graphitic carbon at 1339cm^{-1} and 1586cm^{-1}, respectively. The D-band is assigned to A_{1g} mode and is associated with

the vibrations of carbon atoms with dangling bonds for the in-plane terminations of disordered graphite, i.e. diagnostic of disorder in the carbon structure. The G-band, however, corresponds to the E_{2g} mode of graphite and is related to the vibration of sp^2-bonded carbon atoms in a two-dimensional hexagonal lattice, as in a graphite layer, i.e. diagnostic of structural order [21,22]. The relative intensities of D- and G-bands (I_D/I_G) are commonly used as an index to assess graphitic character. The I_D/I_G ratio was found to be 0.912 (<1) indicating a higher degree of graphitization in the material [21].

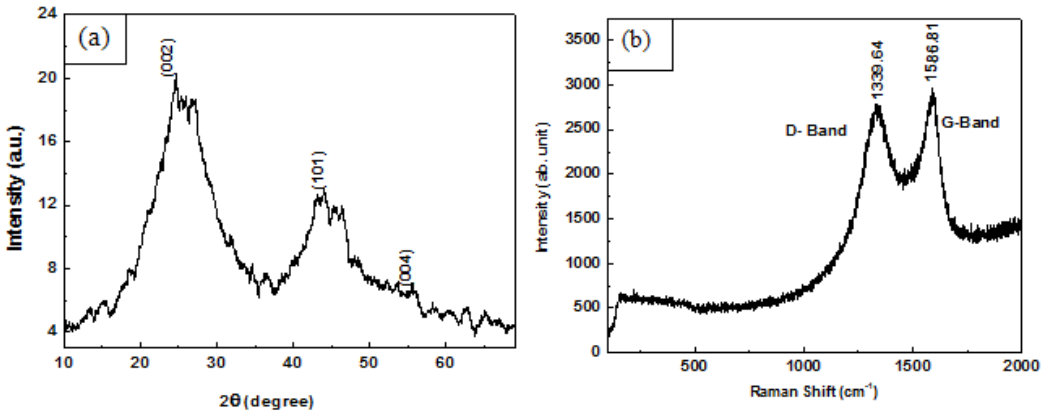

Fig.4.33. (a)XRD pattern **(b)** Raman spectrum of the particles obtained from kanchan flower seed

4.9.Carbon nanoparticles from tishi seed(*Linum usitatissimun)*

4.9.1. Materials

Tishi, commonly known as flax or linseed, with the binomial name *Linum usitatissimum*, is a member of the genus *Linum* in the family Linaceae. It is a food and fiber crop that is grown in cooler regions of the world. The textiles made from flax are known in the West as linen, and traditionally used for bed sheets, underclothes and table linen. The oil is known as linseed oil. Flex seeds are especially rich in protein, dietary fiber, several B vitamins and dietary minerals and Omega 3 (alpha-linolinic acid). The seeds (**Fig.4.34**) were collected from the villages of Hailakandi, Assam, India. After proper washing, drying and crushing, the biomass was used as precursor for the synthesis of nanoparticles.

Fig.4.34. Photographs of **(a)** tishi plant and **(b)** tishiseeds

4.9.2. Synthesis of carbon nanoparticles

Carbon nanoparticles were produced from tishi seed (*Linum usitatissimun)* by pyrolysis in a CVD furnace. Approx. 10g of tishi seed was kept in a quartz boat and inserted into a quartz tube kept in the furnace. Furnace was thoroughly closed and flushed with argon gas for 15 min to flush out the air from the quartz tube. Throughout the pyrolysis as well as during cooling the furnace, the flow of argon was maintained at $6cm^3$/min. The furnace was heated to 800^0C and maintained at that temperature for 2 hours to complete the process of pyrolysis. After cooling the furnace, carbon material was taken out and analyzed as obtained (yield 2.6 g).

4.9.3 Results and discussion

The 'as obtained' carbon nanoparticles black powder is air stable for months and can be dispersed in aqueous and organic solvents (methanol, ethanol) under ultrasonication. The yield of the material was recorded to be around 25% by weight of initial biomass.

4.9.3.1. Transmission electron microscopy

The TEM micrographs(**Fig.4.35)** revealed the presence of agglomeratedparticlesof irregular shape, and their size distribution is also not uniform (50-150nm). The HRTEM image revealed highly crystalline nature of the nanospheres. From HRTEM image **(Fig.4.35(c)),** the lattice fringes were observed to be at interplanar distance of 0.33 nm which correspond to (002) plane of graphitic carbon. The SAED pattern**(Fig.4.35 (d))** indicates polycrystalline nature of the material.

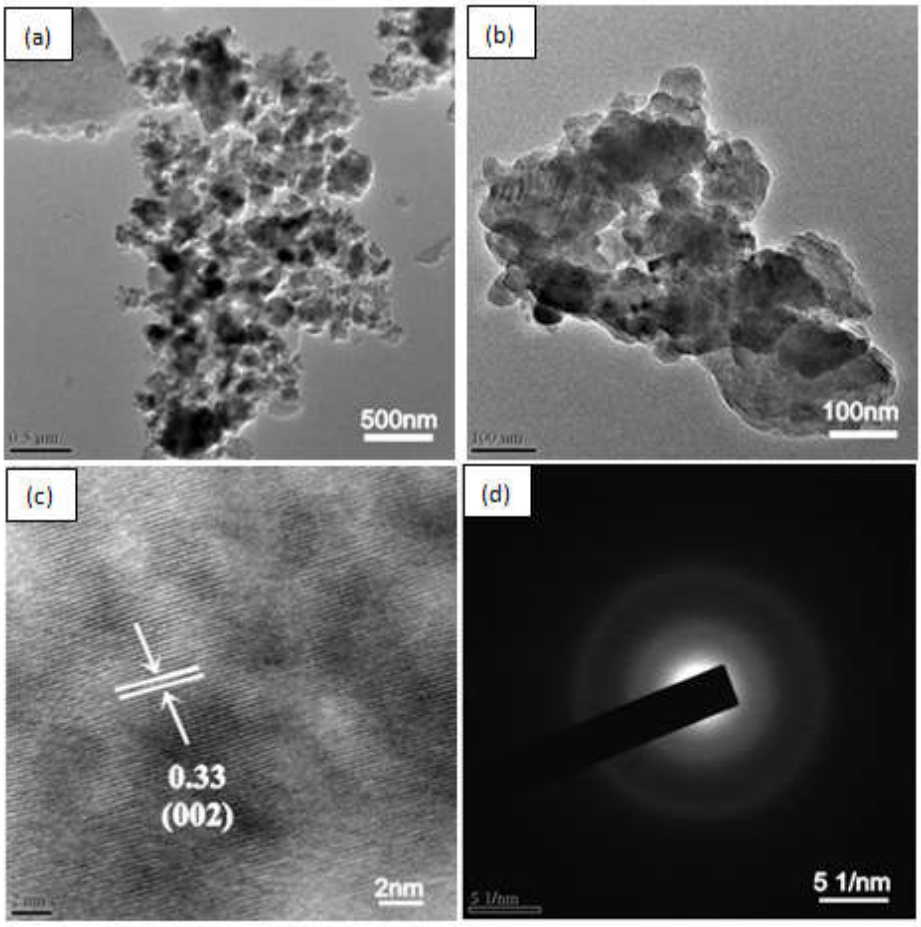

Fig.4.35. (a,b) TEM images **(c)**HRTEM image **(d)** SAED pattern of the materials obtained from tishi seed.

4.9.3.2. XRD analysis

The powder XRD pattern of the as-obtained carbon nanoparticles**(Fig.4.36)** showed major Bragg peaks at 2θ = 25.8^0, 42.5^0, 44.6^0, $50.3^0$and 60.3^0 corresponding to the (002), (100), (101), (102) and (103) planes, respectively of hexagonal graphitic carbon (space group, $P6_3/mmc$, JCPDS Card No. 23-0064). The broad nature of the peak suggests a lesser long range structural order. Interlayer spacing (d=0.33nm) obtained from TEM and a similar value extracted from Bragg's equation evidences a rather high degree of graphitic character of carbon nanoparticles.

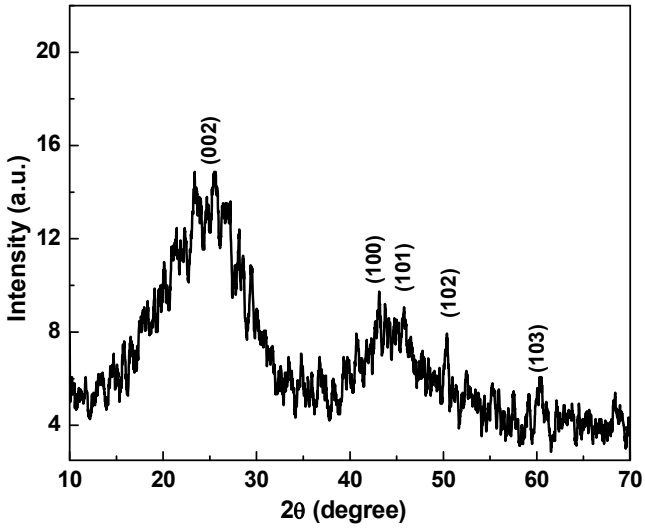

Fig.4.36. XRD patternof the nanoparticles obtained fromtishi plant seeds

4.10. Nanoparticles from seed coat of mahogany(*Swietenia mahogani*)

4.10.1. Materials

Swietenia mahogani, commonly known as mahogany **(Fig.4.37)** is a species of plant in the Meliaceae family. Mahogany is found in almost all the parts of India highly populated in Thattekkad Wildlife Sanctuary, Kaziranga National Park and Corbett National Park. The bark extracts are used as an astringent for wounds. It is also used to cure malaria, anemia diarrhea, fever, dysentery and depurative. Other common uses are in the making of furniture, fixtures, musical instruments, inlay, boat, caskets. Its wood is a very popular material for drum making. The seed coats were collected and processed to use as raw materials for the synthesis of nanoparticles.

Fig.4.37. Photographs of **(a)**mehogony tree and **(b)** mehogony seeds

4.10.2. Synthesis of carbon nanoparticles (CNP)

Carbon nanoparticles were produced seed coats of mehogony (*Swietenia mahogani*) by pyrolysis in a CVD furnace. Approx. 10g of the biomasswas kept in a quartz boat and inserted into a quartz tube kept in the furnace. Furnace was thoroughly closed and flushed with argon gas for 15 min to flush out the air from the quartz tube. Throughout the pyrolysis as well as during cooling the furnace, the flow of argon was maintained at $6cm^3$/min. The furnace was heated to 800^0C at a rate of 7^0C /min and maintained at that temperature for 2 hours to complete the process of pyrolysis. After cooling the furnace, carbon material was taken out and analyzed(yield 2.8 g).

4.10.3. Results and discussion

The 'as obtained' carbon nanoparticles black powder is air stable for months and can be dispersed in aqueous and organic solvents (methanol, ethanol) under ultrasonication. The yield of the material was recorded to be around 30% by weight of initial biomass.

4.10.3.1. Transmission electron microscopy

The TEM image **(Fig.4.38 (a, b))**showed that the nanoparticles are ofirregular shape and their size distribution is also not uniform.The particle size is in the range of 70-200 nm

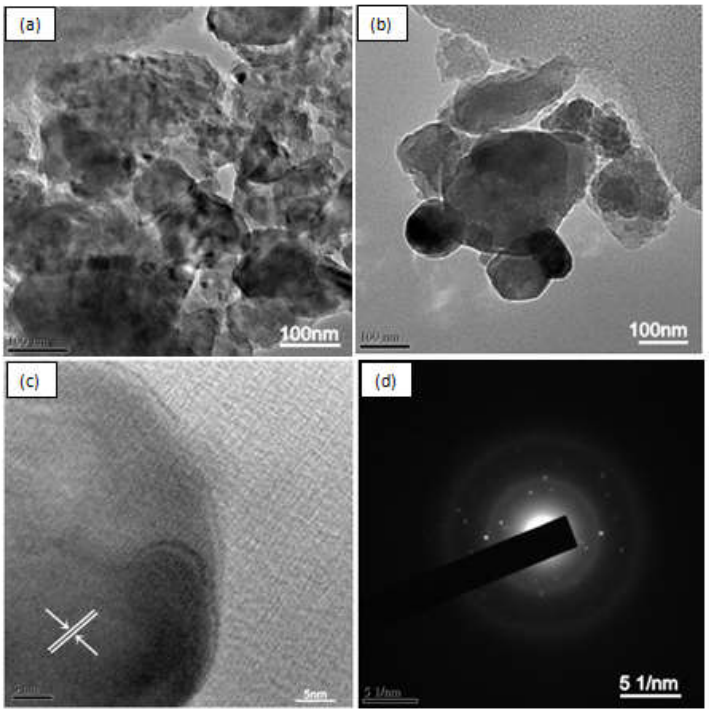

Fig.4.38. (a, b) TEM images **(c)** HRTEM image **(d)** SAED pattern of the nanoparticles obtainedfrom seed coat of mahogany

4.10.3.2. XRD analysis

The powder XRD pattern of carbon nanoparticles obtained by pyrolysis of mahogany seed coat is shown in **(Fig.4.39)**. The diffraction peaks can be well indexed to the hexagonal graphitic carbon (JCPDS Card No. 23-0064). The broad nature of the peak suggests a lesser long range structural order. The average crystallite size estimated Debye-Scherrer formula, using a Gaussian fit was found to be 21nm.

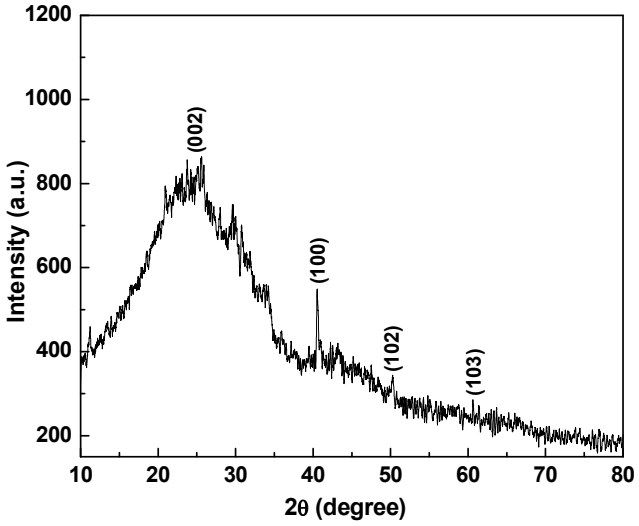

Fig.4.39.XRDpattern of carbon nanoparticles obtained from seed coat of mahogany

References

[1] Bianco, A., Kostarelos, K., & Prato, M. *Curr. Opin. Chem. biol.,* 2005, **9,** 674.

[2] Planeix, J. M., Coustel, N., Coq, B., Brotons, V., Kumbhar, P. S., Dutartre, R., Bernier, P., & Ajayan, P. M. *J. Am. Chem. Soc.,*1994, **116**, 7935.

[3] Darkrim, F. L., Malbrunot, P., & Tartaglia, G. P. *Int. J. Hydrogen Energ.,* 2002, **27**, 193.

[4] Wang, J. *Electroanal,* 2005, **17**, 7.

[5] Zhang, L. L., & Zhao, X. S. *Chem. Soc. Rev.,* 2009, **38**, 2520.

[6] Carrasco, J. A., Prima-Garcia, H., Romero, J., Hernández-Saz, J., Molina, S. I., Abellán, G., & Coronado, E. *J. Mater. Chem. C.,*2016, **4**, 440.

[7] Park, C., & Keane, M. A. *J. Catal.,*2004, **221**, 386.

[8] Zhang, Z., Mu, S., Zhang, B., Tao, L., Huang, S., Huang, Y., Gao, F. & Zhao, Y. *J.Mater. Chem. A.,* 2016, **4**, 2137.

[9] Zhang, P., Qiao, Z. A., & Dai, S. *Chem. Commun*., 2015, **51**, 9246.

[10] Dhand, V., Rao, M. V., Prasad, J. S., Mittal, G., Rhee, K. Y., Kim, H. J., & Jung, D. H. *Carbon Lett*., 2014, **15**, 198.

[11] Rao, C. N. R., Sen, R., Govindaraj, A. *Curr. Opin. Solid State Mater. Sci.,*1996, **1**, 279.

[12] Plonska-Brzezinska, M. E., & Echegoyen, L. *J.Mater.Chem.A*, 2013, **1**, 13703.

[13] Zhang, M. I. N. G., He, D. W., Ji, L., Wei, B. Q., Wu, D. H., Zhang, X. Y., & Wang, W. K. *Nanostruct. Mater.,* 1998,**10**, 291.

[14] Xu, B. S. *New Carbon Mater.,* 2008, **23**, 289.

[15] Reddy, A. L. M., & Ramaprabhu, S. *Nanoscale Res. Lett.*, 2008, **3**, 76.

[16] Wang, Q., Li, H., Chen, L., & Huang, X. *Carbon*, 2001, **39**, 2211.

[17] Liu, X. Y., Huang, B. C., & Coville, N. J. *Carbon*, 2002, **40**, 2791.

[18] Wang, J., Gao, X., Yang, X., Gan, Y., Weng, W., & Gou, Z. *Nanoscale Res. Lett.,* 2009,**4**, 1171.

[19] Khairnar, V., Jaybhaye, S., Hu, C. C., Afre, R., Soga, T., Sharon, M., & Sharon, M. *Carbon Lett.*, 2008, **9**, 188.

[20] Yin, H., Zhou, Y., Meng, X., Shang, K., & Ai, S. *Biosens. Bioelectron.*, 2011, **30**, 112.

[21] Nieto-Márquez, A., Romero, R., Romero, A., & Valverde, J. L. *J. Mater. Chem.,* 2011, **21**, 1664.

[22] Krishnamurthy, G., & Namitha, R. *J. Chil. Chem. Soc*., 2013,**58**, 1930.

[23] Liu, M., Ma, X., Gan, L., Xu, Z., Zhu, D., & Chen, L. *J. Mater. Chem. A.*, 2014, **2**, 17107.

[24] Frackowiak, E. *Phys. Chem. Chem. Phys.,* 2007, **15**, 1774.

[25] Sukeun, P., Jin, P.S., Seok, K, *Carbon Lett.,* 2012, **13**, 130.

[26] Wang, G., Zhang, L., Zhang, *J. Chem Soc Rev.,* 2012, **41**, 797.

[27] Liu, P., Cao, Y. L., Wang, C. X., Chen, X. Y., & Yang, G. W.*NanoLett.,* 2008, **8**, 2570.

[28] Sun, Y. P., Zhou, B., Lin, Y., Wang, W., Fernando, K. S., Pathak, P. Meziani, M.J., Harruff, B.A., Wang, X., Wang, H.,& Luo, P. G. *J. Am. Chem. Soc.*, 2006, **128,** 7756.

[29] Cao, L., Wang, X., Meziani, M. J., Lu, F., Wang, H., Luo, P. G. Lin, Y., Harruff, B.A., Veca, L.M., Murray, D.& Xie, S. Y. *J. Am. Chem. Soc*., 2007, **129**, 11318.

[30] Sonkar, S. K., Saxena, M., Saha, M., Sharkar, S., *J. Nanosci. Nanotechnol.*, 2010, **10**, 4064.

[31] Thompson, B. C., & Frechet, J. M. *Angew. Chem. Int. Ed.*, 2008**, 47,** 58.

[32] Park, S. H., Roy, A., Beaupre, S., Cho, S., Coates, N., Moon, J. S.,Moses, D., Leclerc, M., Lee, K.& Heeger, A. J. *Nature Photon.,* 2009,**3**, 297.

[33] Spanggaard, H., & Krebs, F. C. *Sol. Energ. Mat. Sol. Cells.,* 2004,**83**, 125.

[34] Dennler, G., Scharber, M. C., & Brabec, C. J. *Adv. Mater.,*2009, **21**, 1323.

[35] Du Pasquier, A., Unalan, H. E., Kanwal, A., Miller, S., & Chhowalla,M. *Appl. Phys. Lett.*, 2009,**87**, 203511.

[36] Kim, Y. K., & Min, D. H. *Langmuir*, 2009, **25**, 11302.

[37] Hecht, D. S., Hu, L., & Irvin, G. *Adv. Mater.*, 2011, **23**, 1482.

[38] Sun, Y., Wu, Q., & Shi, G. *Energ. Environ. Sci.*, 2011, **4**, 1113.

[39] Candelaria, S. L., Shao, Y., Zhou, W., Li, X., Xiao, J., Zhang, J. G., Wang, Y., Liu, J., Li, J. & Cao, G. *Nano Energy,* 2012, **1**, 195.

[40] Largeot, C., Portet, C., Chmiola, J., Taberna, P. L., Gogotsi, Y., & Simon, P.*J. Amer. Chem. Soc.*,2008, **130,** 2730.

[41] Amitha, F. E., Reddy, A. L. M., & Ramaprabhu, S. *J. Nanopart. Res*., 2009, **11,** 725.

[42] Galano, A. *Nanoscale,* 2010, **2**, 373.

[43] Qiu, Y., Wang, Z., Owens, A. C., Kulaots, I., Chen, Y., Kane, A. B., & Hurt, R. H. *Nanoscale*, 2014, **6**, 11744.

[44] Edge, R., McGarvey, D. J., & Truscott, T. G. *J. Photochem. Photobiol. B*, 1997, **41**, 189.

[45] Serpen, A., Capuano, E., Fogliano, V., Gokmen, V. *J. Agric. Food Chem.*, 2007, **55**, 7676.

[46] Brand-Williams, W., Cuvelier, M. E., & Berset, C. *LWT-Food Sci. Technol.*, 1995, **28**, 25.

[47] Naik, G. H., Priyadarsini, K. I., Satav, J. G., Banavalikar, M. M., Sohoni, D. P., Biyani, M. K., & Mohan, H. *Phytochemistry*, 2003, **63**, 97.

[48] Kumar, R., Tiwari, R. S., & Srivastava, O. N. *Nano*, 2011, 6, 215

[49] Sharon, M., Soga, T., Afre, R., Sathiyamoorthy, D., Dasgupta, K., Bhardwaj, S. Sharon M. & Jaybhaye, S. *Int. J. Hydrogen Energ.,* 2007,**32**, 4238.

[50] Xiao, Q., & Zhou, X. *Electrochim. Acta*, 2003, **48**, 575.

[51] Frackowiak, E., Metenier, K., Bertagna, V., & Beguin, F. *Appl.Phys. Lett*., 2000,**77**, 2421.

[52] Babel, K., & Jurewicz, K. *J. Phys. Chem. Solids.*2004, **65**, 275.